© 2018. Published by The Company of Biologists Ltd | Development (2018) 145, dev161083. doi:10.1242/dev.161083

RESEARCH ARTICLE

In locus analysis of patterning evolution of the BMP type II receptor Wishful thinking

Robert A. Marmion[1,*] and Nir Yakoby[1,2,‡]

ABSTRACT

Proper tissue patterning is an essential step during organ formation. During this process, genes are expressed in distinct patterns, defining boundaries for future functional domains. The bone morphogenetic protein (BMP) signaling pathway sets the anterior domain during eggshell patterning. Previously, the *Drosophila melanogaster* homolog of BMPR2, Wishful thinking (WIT), was shown to be required for BMP signaling and patterning during eggshell formation. Expressed in a conserved anterior pattern, the width of *wit* patterning in the follicular epithelium is evolutionarily divergent between *Drosophila* species. We used genome editing to demonstrate how the gene pattern divergence is controlled in *cis* within the *wit* locus of *D. virilis*. Furthermore, unlike direct targets of BMP signaling, we demonstrate how one transcription factor binding site shapes the pattern of WIT in *D. melanogaster* by negative regulation. However, changes in this site are not sufficient to explain the evolution of *wit* patterning, suggesting that a positive regulatory element that controls pattern divergence remains to be discovered.

KEY WORDS: Tissue patterning, Oogenesis, TGFβ signaling, *Drosophila*

INTRODUCTION

Boundary formation is a fundamental requirement during animal development (Dahmann et al., 2011). In tissues, a handful of cell-to-cell signaling pathways inform cells of their position. Consequently, cells acquire different fates in order to form organs (Ashe and Briscoe, 2006; Hamaratoglu et al., 2014; Moussian and Roth, 2005; Wolpert, 1989). In the *Drosophila* ovaries, eggs are produced in an assembly line manner (Bastock and St Johnston, 2008; Hinton, 1981; Horne-Badovinac and Bilder, 2005; Spradling, 1993). During egg development, numerous cell signaling pathways, including the epidermal growth factor receptor (EGFR) and bone morphogenetic protein (BMP) signaling, control the dorsal-ventral and anterior-posterior axes of the fly (Berg, 2005; Deng and Bownes, 1997; Moussian and Roth, 2005; Neuman-Silberberg and Schupbach, 1994; Peri and Roth, 2000; Yakoby et al., 2008b). The BMP2/4 ligand homolog in *Drosophila*, Decapentaplegic (Dpp), activates the BMP pathway through a heteromeric complex of type I and type II receptors (Parker et al., 2004; Raftery and Sutherland, 1999; Wu and Hill, 2009). Previous work focused largely on the necessity and patterning of the BMP type I receptor Thickveins (Mantrova et al., 1999; Niepielko et al., 2011, 2012). Wishful thinking (Wit) was identified as the BMP type II receptor in the follicle cells of *D. melanogaster* (Marmion et al., 2013; Yakoby et al., 2008a). It was shown to be necessary for signaling and proper patterning of the eggshell. Here, we focus on gene patterning during oogenesis.

One way to identify common mechanisms of gene regulation is to search for overlapping spatiotemporal expression domains (Konikoff et al., 2012; Kumar et al., 2017). In *D. melanogaster*, the anterior domain of the follicular epithelium is patterned by BMP signaling (Twombly et al., 1996). Numerous genes are expressed in the anterior domain of the follicle cells (Jordan et al., 2005; Peri and Roth, 2000; Twombly et al., 1996; Yakoby et al., 2008b). The BMP inhibitor gene *Daughters against dpp* (*Dad*) is a known target of BMP signaling in the imaginal wing discs and the follicle cells (Marmion et al., 2013; Weiss et al., 2010). This gene is regulated directly by the activated intracellular BMP signaling transducer complex P-Mad/MED. At the same time, *dpp* is also expressed in an anterior pattern that is strikingly similar to the expression pattern of *Dad* (Twombly et al., 1996). However, *dpp* is not regulated by BMP signaling; rather, it is regulated by a combination of the EGFR and Janus kinase/signal transducer and activator of transcription (JAK/STAT) pathways (Peri and Roth, 2000; Xi et al., 2003). This was recently confirmed by *cis*-regulatory module (CRM) analysis screening using the FlyLight collection (Revaitis et al., 2017). The *Dad* CRM responded to ectopic BMP signaling, whereas the *dpp* CRM did not. This raises the following question: Are all genes expressed in the anterior domain regulated by the same mechanism?

The expression of *wit* is maintained in a positive-feedback loop at the anterior domain of the follicular epithelium (Marmion et al., 2013). However, the precise nature of the regulatory mechanism is not completely understood. Motivated by the subtle differences in the anterior pattern of *wit* across *Drosophila* species, we aimed to dissect the nucleotide-level changes in the regulatory domain of *wit* patterning between two fly species. We used CRISPR/Cas9 gene editing to test changes within the genomic context of *wit* in *D. melanogaster*. We found that *wit* is regulated indirectly by BMP signaling through the alleviation of Brinker (BRK) repression. This mechanism is maintained in *D. virilis*, a species that is separated from *D. melanogaster* by 45 million years. We recapitulated the local arrangement of other potential binding sites from *D. virilis* within *D. melanogaster*, but, surprisingly, this did not affect WIT expression. We conclude that a yet undiscovered positive element is changed between these two species.

RESULTS

The anterior pattern of *wit* is diverse and regulated in *cis*

In *D. melanogaster*, *wit* is expressed in a band of cells that is on average 2.4±0.1 (mean±s.e.m.) cells wide (Fig. 1A) (Yakoby et al., 2008a). The corresponding P-Mad pattern at stage 10A is on average 1.7±0.1 (mean±s.e.m.) cells wide (Fig. 1B). Previously, we

[1]Center for Computational and Integrative Biology, Rutgers, The State University of NJ, Camden, NJ 08102, USA. [2]Department of Biology, Rutgers, The State University of NJ, Camden, NJ 08102, USA.
*Present address: The Lewis-Sigler Institute for Integrative Genomics, Princeton University, Princeton, NJ 08544, USA.

‡Author for correspondence (yakoby@camden.rutgers.edu)

R.A.M., 0000-0002-3895-0584; N.Y., 0000-0002-7959-7588

Received 27 October 2017; Accepted 29 May 2018

Development (2018) 145, dev161083. doi:10.1242/dev.161083

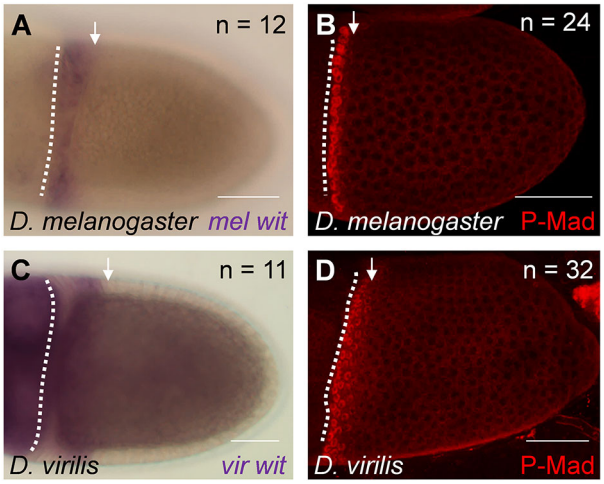

Fig. 1. The pattern of *wit* is different in *D. melanogaster* and *D. virilis*. (A) The *wit* gene in *D. melanogaster* is expressed in an anterior band approximately two cells wide (arrow). (B) P-Mad is detected in a similar band (arrow), two cells wide. (C) The *wit* gene in *D. virilis* is expressed in a pattern approximately four cells wide (arrow). (D) P-Mad is also detected in this expanded domain (arrow). In all panels, anterior is to the left. Dotted white line denotes the anterior boundary of the oocyte-associated follicle cells. *n*, number of egg chambers scored with a similar pattern. Scale bars: 50 µm.

demonstrated the conservation of this simple expression pattern in closely related species, including *D. sechellia* and *D. simulans* (Marmion et al., 2013). We hypothesized that in more evolutionarily divergent species of *Drosophilid*, we might find different patterns of *wit*, as has been shown for the type I BMP receptor *thickveins* (*tkv*) (Niepielko et al., 2011, 2012). We selected *D. virilis* to test patterning changes, which accounts for ∼45 million years of evolution. We found that not only was *wit* patterning wider (Fig. 1C) but it is correlated with changes in the width of P-Mad in this species (Fig. 1D). Specifically, *wit* is expressed in a band that is 4.8±0.2 (mean±s.e.m.) cells wide on average. The P-Mad pattern band had an average width of 3.0±0.1 (mean±s.e.m.) cells. These are both significantly different from the corresponding expression patterns in *D. melanogaster* (P=3.3×10^{-14} and 1.4×10^{-10}, respectively).

The *D. virilis wit* locus rescues a CRISPR null allele of Wishful thinking

Intrigued by the wider expression pattern of *wit* in *D. virilis*, we aimed to understand whether the patterning change is regulated in *cis* or is unique to *D. virilis* and thus regulated in *trans*. To examine the mechanism of gene patterning within the endogenous context, we engineered a knockout allele of *wit* (Fig. 2A, Fig. S1). We replaced the entire *wit* locus in *D. melanogaster* with a ϕC31 site, including most of the previously identified follicle cell-associated *wit* enhancer (only 217 bp remaining out of 1261 bp of witZ) (Marmion et al., 2013). Importantly, as we show later in Fig. 3, a functional short fragment of witZ, which we name wit6 (Fig. 3E,F), was completely removed (Fig. 2A, Figs S1 and S2). This ϕC31 site served as a hub for genetic modification within the *wit* locus (Fig. 2B). The recovered knockout allele of *wit* is homozygous lethal; pharate adults fail to eclose from the pupal casings (Fig. S1C), consistent with other null alleles of *wit* (Aberle et al., 2002; Marqués et al., 2002).

First, we generated a construct that contained the wild-type *wit* locus from *D. melanogaster*, which was inserted into the ϕC31 site. This allele is homozygous viable and reproduced the wild-type anterior pattern of WIT (Fig. 2D). Also, a CFP-tagged *wit* was able

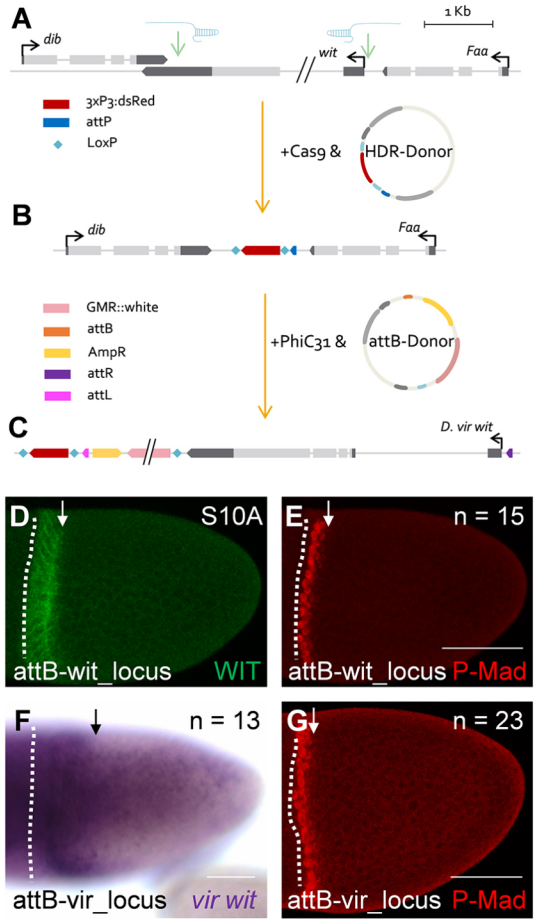

Fig. 2. The *D. virilis wit* locus rescues a *wit* null *D. melanogaster* fly. (A) Schematic of the method for *in locus* gene replacement with attP landing site. (B) Upon homologous recombination, the attP site is inserted along with a positive selection cassette of 3xP3:dsRed. (C) The *D. virilis wit* locus is inserted into *D. melanogaster wit* locus via ϕC31 insertion. (D,E) The null *wit* locus in *D. melanogaster* is rescued by insertion of the wild-type *wit* locus from *D. melanogaster*, which results in anterior expression of WIT (D) and two-cell-wide expression of P-MAD (E). (F) *In situ* hybridization for the *D. virilis wit* mRNA in *D. melanogaster* (the fly generated in C) is similar to the wild-type expression of *wit* in *D. virilis* (Fig. 1C). (G) P-MAD expression detected in the anterior region is two cells wide. In all images, anterior is to the left. Dotted white line denotes the anterior boundary of the oocyte-associated follicle cells. *n*, number of egg chambers scored with a similar pattern. Arrows in D-G mark the expression boundary. Scale bars: 50 µm.

to rescue the null fly (Fig. S3). The corresponding pattern of P-Mad was detected in a band of an average of 1.9±0.1 (mean±s.e.m.) cells wide (Fig. 2E), which was not significantly different from OreR (P=0.34) (Fig. 1B). Next, we created a construct that includes the entire *wit* locus from *D. virilis* (Fig. 2C), and tested whether it can rescue a *D. melanogaster wit* null fly. This construct was targeted to the ϕC31 site in the *wit* locus. Consistent with the endogenous pattern of *wit* in *D. virilis* (Fig. 1C), the vir-*wit* was expressed in an anterior pattern of 4.4±0.2 (mean±s.e.m.) cells wide in addition to a low level of uniform expression (Fig. 2F). This suggests that the regulatory elements of vir-*wit* are included in this locus and the differences between the species are changes in *cis*. Surprisingly, unlike the wide pattern of P-Mad in *D. virilis* (Fig. 1D), the P-Mad domain is similar to the pattern found in *D. melanogaster* (Fig. 1D and Fig. 2G) (Yakoby et al., 2008b). We reason that the anteriorly secreted DPP ligands bind to a uniformly expressed TKV (Mantrova et al., 1999; Yakoby et al., 2008b) and

Development (2018) 145, dev161083. doi:10.1242/dev.161083

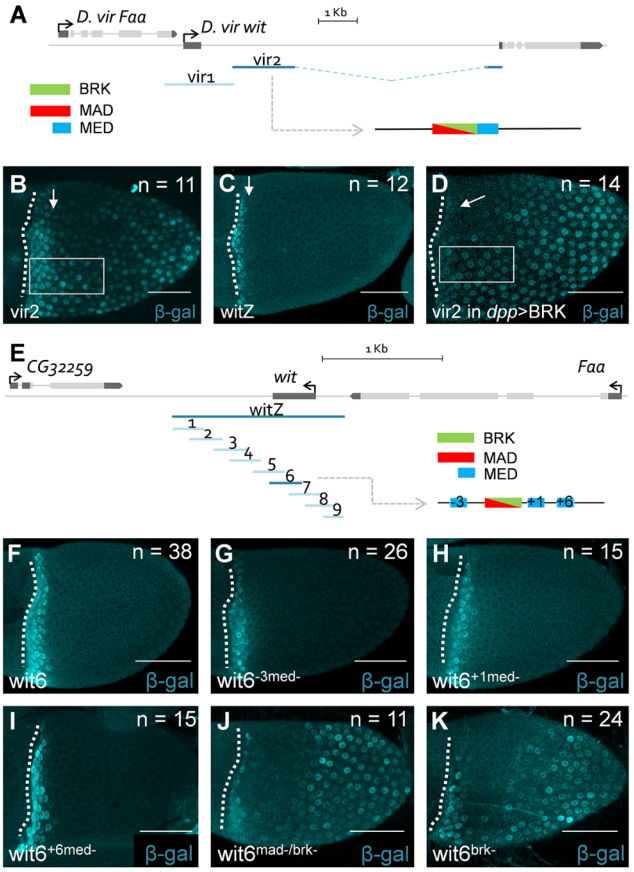

Fig. 3. The *wit* enhancers of both *D. melanogaster* and *D. virilis* are repressed by a BRK binding site. (A) Schematic of the *D. virilis* test enhancers in the *wit* locus. The BRK/MAD site is flanking the MED binding site. (B) vir2-LacZ, which contains a BRK/MAD consensus binding site, drives expression of *lacZ* in *D. melanogaster* weakly uniform and strongly in an anterior pattern, approximately four cells wide (arrow). (C) The witZ enhancer from *D. melanogaster* drives expression in a band approximately two cells wide (arrow). (D) The high-level expression of the anterior pattern of vir2-LacZ is repressed in the follicle cells by ectopic expression of BRK by *dpp*-GAL4. Boxes in B and D mark the area of intensity measurements. White arrow denotes the dorsal anterior domain of vir2-LacZ expression in the wild type (B) and *dpp*-GAL4>BRK (*dpp*>BRK) (D). (E) Schematic of the *D. melanogaster* test enhancers in the *wit* locus. All nine overlapping fragments cover entirely the previously characterized witZ enhancer (Marmion et al., 2013). The positions of the predicted three MED binding sites are marked relative to the BRK/P-Mad binding site (−3, +1, +6). (F) wit6 containing a BRK/P-Mad consensus site drives expression two or three cells wide in the anterior. (G-I) Elimination of any of the three MED sites leads to a wild type-like anterior pattern. (J) Elimination of P-Mad and BRK binding sites leads to a uniform expansion of the pattern. (K) Elimination of only BRK binding causes uniform expression. In both J and K, reduced expression is seen in the dorsal anterior. In all images, anterior is to the left. Dotted white line denotes the anterior boundary of the oocyte-associated follicle cells. Number of egg chambers scored with a similar pattern are denoted by *n*. Scale bars: 50 µm.

the anteriorly expressed vir-WIT; consequently, BMP signaling is activated proximal to the DPP source.

Expression of *wit* is regulated by alleviation of Brinker repression

Following up on the pattern of vir-*wit* in *D. melanogaster*, we sought to determine the mechanism underlying *wit* regulation. We screened two potential enhancers from *D. virilis* using a *lacZ* reporter in *D. melanogaster* (Fig. 3A). The Brinker (BRK, GGCGYY) and phosphorylated Mothers against DPP (P-Mad, GRCGNC) binding sites have much in common (Hamaratoglu et al., 2014; Zhang et al., 2001). We characterized two fragments that contain a BRK/P-Mad binding site (GGCGCC). The first fragment tested (vir1) failed to produce any expression in the follicle cells (not shown). However, the second enhancer tested (vir2) produced expression that had a distinct wide anterior expression pattern on top of a uniform background expression (Fig. 3B). This pattern is similar to the endogenous pattern of vir-*wit* in *D. virilis* and *D. melanogaster* (Fig. 1C and Fig. 2F), but different from the anteriorly restricted pattern of the previously characterized 1.26 kb fragment of the *wit* enhancer (witZ) from *D. melanogaster* (Fig. 3C) (Marmion et al., 2013).

Target genes of BMP signaling are regulated by direct binding of the P-Mad/MEDEA (P-Mad/MED) complex or by repression of the transcriptional inhibitor BRK (Kirkpatrick et al., 2001; Müller et al., 2003; Pyrowolakis et al., 2004; Weiss et al., 2010). The vir2 enhancer contains only one MED site adjacent to the BRK/P-Mad site (there are no nucleotides between the predicted P-Mad and MED binding sites) (Fig. 3A). The previously described activation/silencer element (AE/SE) requires a nucleotide linker of 5 nt. Although this linker length is variable, a linker as short as 3 nt reduces binding considerably (Pyrowolakis et al., 2004). Based on the position of the MED binding site in the vir2 enhancer in relation to the position of the BRK/P-Mad binding site, we did not expect that the P-Mad/MED complex would be able to bind and activate expression through this site (Weiss et al., 2010) and would instead be regulated by BRK. Measured laterally, the intensity of the vir2 anterior band was 70±4.3 a.u. (mean±s.e.m.) and the uniform level was 36±1.1 a.u. (mean±s.e.m.) (Fig. 3B). At the same time, in the *dpp*>BRK background, the anterior band was decreased to 44±3.0 a.u. (mean±s.e.m.) and the uniform level was 32.5±1.7 a.u. (mean±s.e.m.) (Fig. 3D). We note that the intensity of anterior expression of vir2 in the *dpp*>BRK background (Fig. 3D) was reduced compared with the wild type (Fig. 3B) (P=0.0002). As expected, the intensity of uniform expression remained unchanged (P=0.08). On the dorsal anterior side, the approximately four-cell-wide band of vir2 expression was reduced to an approximately one-cell-wide fragmented band (Fig. 3B,D). These results further support the role of BRK repression in the regulation of the *D. virilis wit* gene. Our attempts to separate this enhancer to three smaller fragments did not produce expression (not shown).

We previously reported that *brk* mutant clones did not lead to detectable WIT expression in *D. melanogaster* (Marmion et al., 2013). This suggests that in *D. melanogaster*, *wit* is regulated by P-Mad/MED binding. To compare between the enhancers from the two species, we aimed to dissect further the regulation of *wit* in *D. melanogaster*. We divided the witZ into nine smaller fragments (Fig. 3E). The consensus between BRK and P-Mad is largely overlapping, so the regulation could be through the contribution of MED binding sites and/or the competition between BRK and P-Mad binding. The average size of each of the nine fragments covering witZ is ∼240 bp (Fig. 3E). Of all tested fragments, only fragment 6 (wit6) generates a pattern that is similar to the witZ pattern (Fig. 3F). The wit6 fragment contains an exact match to the BRK/P-Mad binding site (GGCGCC).

Based on the assumption that *wit* is positively regulated by BMP signaling (Marmion et al., 2013), we investigated the role of proximal MED sites (GNCN) in regulation of the proper gene patterning of *wit*. Three predicted MED binding sites exist proximal to the BRK/P-Mad site; N-nucleotide spacers of −3, +1 and +6 are found within wit6 (Fig. 3E). Based on our previous analysis of witZ (Marmion et al., 2013), we were surprised that mutation of any of the three MED sites did not perturb the expression pattern (Fig. 3G-I). We next mutated

Development (2018) 145, dev161083. doi:10.1242/dev.161083

the BRK/P-Mad site in order to reduce binding of both factors, expecting to lose or considerably reduce expression. However, we were surprised to find a uniform expansion of the tested enhancer (Fig. 3J). Next, we tested this further by mutating only the BRK binding (P-Mad binding is still present). The uniform expansion remained (Fig. 3K). These results support an alternative regulation mechanism by the BMP negative regulator BRK (Hamaratoglu et al., 2014), similar to what was found for vir2.

Expression divergence is not regulated by differences in the Brinker binding site

The enhancer analysis is contrary to our previous analysis of *brk* null clones that failed to detect an increase in *wit* expression (Marmion et al., 2013). Thus, we aimed to resolve this discrepancy. The pattern of P-Mad and BRK expression is found in anti-correlated graded domains (Fig. 4A-C). We repeated experiments for *brk* clones; however, this time, we halved the time of dissection and permeabilization during the immunohistochemistry procedure (see Materials and Methods for more details). Under these modified conditions, we detected WIT in cells null for *brk* (Fig. 4D,F). We reason that the stability of WIT in various regions of the follicle cells is different. By reducing the time from dissection to fixation, the levels of WIT were above the detection level. We did not detect changes in the P-Mad pattern in this perturbation (Fig. 4E).

To further explore the regulation of *wit* by BRK, we utilized the ϕC31 site in the *wit* locus (Fig. 2) to test specific modifications in the binding sites within the *wit* locus (Fig. 4G, Fig. S4). Consistent with our prediction of patterning by BRK, complete removal of the BRK binding site resulted in a uniform high expression of WIT (Fig. 4H). P-Mad was detected in a band of 2.2±0.1 (mean±s.e.m.) cells wide on average, similar to the wild-type pattern (Fig. 1B). In about 12% of the egg chambers, the removal of this site also resulted in ectopic detection of P-Mad (Fig. 4I,I′). Interestingly, this allele is homozygous viable and generated no changes in eggshell morphologies. Unlike ectopic expression of the type I receptor TKV, which mainly restricts DPP diffusion and consequently confines signaling near the ligand source (Crickmore and Mann, 2006; Niepielko et al., 2012), ectopic expression of the type II receptors (WIT and/or Punt) led to activation of BMP signaling (not shown). We reason that the levels of ectopic WIT expression were sufficient to activate the pathway above the detection limit. In this case, a complete removal of the BRK binding site was sufficient to increase the levels of *wit* expression, and consequently increase BMP signaling levels above the detection limit within a portion of the egg chambers (Fig. 4I′).

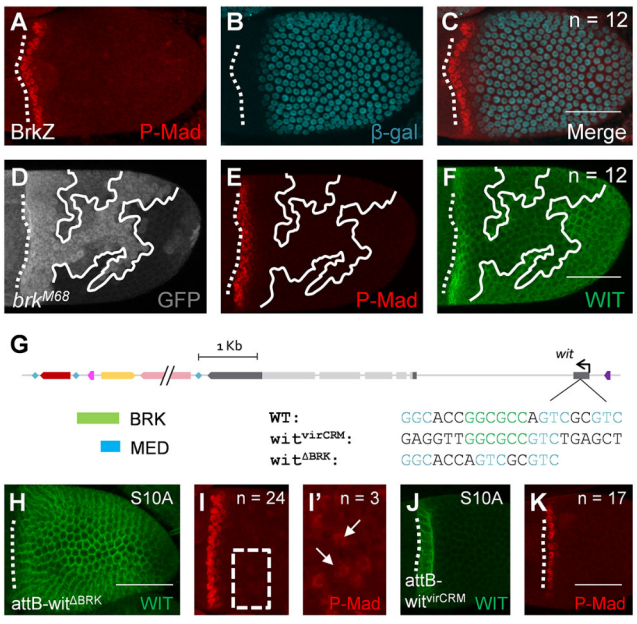

Fig. 4. *wit*/WIT patterning in the follicle cells depends on BRK. (A-C) The pattern of P-Mad (A) and expression of BRK-LacZ reporter (B) in wild-type *D. melanogaster* and merged image of A and B (C) showing that P-Mad and BRK are present in mutually exclusive domains. (D) Cells null for *brk* are marked by loss of GFP (solid white outline). (E) *brk* null cells do not contain ectopic P-Mad. (F) *brk* null cells ectopically express WIT. (G) Schematic of *D. melanogaster* replacements of modified *wit* enhancers. (H,I) The null *wit* locus is rescued by the insertion of a *wit* with a removed BRK binding site, which results in uniform expression of WIT (H) and P-Mad in the anterior (I). (I′) Magnification of the boxed region in I showing ectopic P-Mad away from the anterior (white arrows). (J,K) The null *wit* locus is rescued by insertion of *wit* with a CRM from *D. virilis*, which results in anterior expression of WIT (J) and P-Mad in the anterior (K). In all images, anterior is to the left. Dotted white line denotes the anterior boundary of the oocyte-associated follicle cells. Number of egg chambers scored with a similar pattern are denoted by *n*. Scale bars: 50 µm.

The noteworthy differences in the CRMs for *D. melanogaster* and *D. virilis* are the number of MED binding sites and their proximity to the BRK/P-Mad site (Fig. 3A,E). As shown above, *wit* is regulated by BRK in both species. However, we aimed to determine whether the patterning divergence between the two species depends on the proximal environment of the BRK/P-Mad binding site. We replaced the BRK/P-Mad/MED site in *D. melanogaster*, which spans 21 nucleotides, with 21 nucleotides that are proximal to the BRK/P-Mad site in *D. virilis* (Fig. 3A and Fig. 4G). This virCRM allele is homozygous viable and WIT expression was a similar width to that induced by the wild-type rescue construct (P=0.79) (Fig. 4J). The P-Mad width was consistent with WIT expression with a pattern that was 1.8±0.1 (mean±s.e.m.) cells wide (Fig. 4K). Thus, the sequence around the BRK/P-Mad site in *D. virilis* cannot account for the difference in WIT patterning between species.

DISCUSSION

The anterior patterning of the follicle cells seems simple (Yakoby et al., 2008a); however, various mechanisms control this process. The BMP inhibitor *Dad* is regulated directly by BMP signaling in the imaginal wing discs and the follicle cells (Marmion et al., 2013; Weiss et al., 2010). At the same time, *dpp* expression is regulated by a combination of the EGFR and JAK/STAT pathways (Peri and Roth, 2000; Xi et al., 2003). This was recently confirmed by a CRM analysis screen using the FlyLight collection (Revaitis et al., 2017). The same screen found additional CRMs with different extents of anterior coverage, including an anterior portion of the stretched cells, all stretched cells, and stretched cells and centripetally migrating follicle cells. This suggests additional complexity in the regulation of genes in the anterior domain. Identifying these CRMs opens an opportunity to answer whether additional mechanisms control the anterior patterning of the follicle cells.

The vir2 enhancer controls a wide anterior expression pattern of the reporter, in addition to a lower uniform pattern throughout the follicle cells (Fig. 3B). However, replacing the 21 nucleotides proximal to the BRK binding site of *D. virilis* in the context of *D. melanogaster* generated an anterior pattern of WIT that is indistinguishable from the endogenous pattern of WIT in *D. melanogaster* (Fig. 4J). In this case, the vir2 fragment contains additional information for a uniform expression that is independent of the predicted BRK binding site. This type of uniform expression during oogenesis is common to other genes, including the early patterns of *wit*, *thickveins* (*tkv*) and *br*

Development (2018) 145, dev161083. doi:10.1242/dev.161083

(Deng and Bownes, 1997; Fuchs et al., 2012; Mantrova et al., 1999; Marmion et al., 2013; Yakoby et al., 2008a,b). The early expression of *br* was shown to be regulated by Notch signaling (Jia et al., 2014), but the regulator of uniform expression is still unknown. Interestingly, these patterns are dynamically regulated at later stages of development. Although the three genes remain in an overlapping pattern in the ventral anterior domain of the follicle cells, *br* and *tkv* also appear on the dorsal side as two patches on either side of the dorsal midline (Deng and Bownes, 1997; Fuchs et al., 2012), and *wit* becomes absent from the dorsal anterior domain. The dorsal repression of *wit* is likely to be due to high levels of BRK induction as a result of activation of EGFR signaling in the dorsal anterior domain (Chen and Schüpbach, 2006). The wit^{brk-} reporter drives patchy dorsal anterior expression (Fig. 3K), which may indicate that the modified BRK binding site can still bind BRK, especially at the dorsal anterior domain where BRK expression is highest. Further support for this assumption is the uniform expression of WIT in the follicle cells when the BRK binding site is completely removed (Fig. 4H). We hypothesize that an as-yet-uncharacterized transcriptional activator has stronger or more abundant binding sites within the *D. virilis* CRM, accounting for the *cis* changes in the anterior pattern.

The eggshells of *D. melanogaster* and *D. virilis* differ in several aspects of their morphology, including the number of respiratory dorsal appendages (two and four, respectively), and a larger operculum in *D. virilis* (Niepielko et al., 2011). The wider anterior pattern of P-Mad in *D. virilis* was reasoned to be due to the late uniform expression of TKV, in contrast to the anterior clearing of TKV in *D. melanogaster*. Here, although WIT is uniformly expressed when the BRK binding site is removed, it still does not change the pattern of P-Mad or eggshell morphologies. In the future, it will be interesting to determine whether the uniform expression of both WIT and TKV in *D. virilis* is required for the expansion of the P-Mad domain as well as the operculum size.

MATERIALS AND METHODS

Fly stocks

Oregon R (OreR) Bloomington #25211 was utilized as wild type for *D. melanogaster*. *D. virilis* was provided by the *Drosophila* Species Stock Center at UC San Diego (stock #15010-1051.88). Clonal analysis of Brinker was conducted using the Flp/*FRT* system (Theodosiou and Xu, 1998) utilizing: FRT^{19A} BRK^{M68}/FRT^{19A} ubiGFP; e22c-GAL4 UAS-flp. A UAS-BRK (a gift from J. Duffy, Worcester Polytechnic Institute, MA, USA) was expressed with the oogenesis dpp:GAL4 driver (Revaitis et al., 2017). The trap *lacZ* of Brinker was used to mark BRK expression (X47[PlacZ(ry+)]) (Campbell and Tomlinson, 1999). All other fly stocks were generated for this study. Four- to seven-day-old flies were used in this study. Only female flies were dissected.

Creation of *wit* reporters

witZ1-9 fragments were amplified in pairs of forward and reverse primers and cloned into a gateway entry vector, PCR8. For the *D. virilis* enhancers, split1 was amplified with vir_big_F and vir_split1_R, and split2 was amplified with vir_split2_F and vir_small_R. The full sequences of the corresponding primers can be found in Table S1. As reported previously, prospective enhancers were subcloned into a *lacZ* reporter vector by Gateway reaction and inserted by ϕC31 injection into the genomic site attP2 at 68A4 of chromosome III (Marmion et al., 2013).

Creation of a *wit* null allele

Two CRISPR targets were chosen that cut the *wit* locus within the 3′ UTR and in the upstream intergenic region using online prediction software (Housden et al., 2015; Ren et al., 2013). CRISPR chiRNAs were cloned into U6-chiRNA (Gratz et al., 2014). This was achieved by annealing sense and antisense unphosphorylated oligos at 10 µM in ligation buffer with the following thermocycler settings: 95°C for 5 min, then ramping to 25°C at a rate of −0.1°C/s. Annealed oligos were diluted (1:100) and 30 fmol of each chiRNA were ligated to 10 fmol of vector that had been digested with *Bbs*I [New England Biolabs (NEB), R3539S], excluding the dephosphorylation step in a 10 µl reaction (cttcGTCTTGGACAAGAGCGAAAC and aaacGTTTCGCTCTTGTCCAAGAC, cttcGCGCTCAGCTATGCTCCCAT and aaacATGGGAGCATAGCTGAGCGC). Similarly, homology arms were amplified such that they were directly adjacent to the CRISPR cut sites. Homology arms were cloned into pdsRed_attP using cloning sites *Aar*I (Thermo Fisher Scientific, ER1581) and *Sap*I (NEB, R0569S) in subsequent cloning/transformation reactions. Flies containing a nos:Cas9 in the attP40 site of chromosome II were injected with a mixture of all three plasmids by Rainbow Transgenic Flies. Flies positive for repair by homology directed repair had red glowing eyes (dsRed). PCR confirmation of a heterozygous knockout was confirmed by mixture of primers wit_crispr_conf_left, wit_crispr_conf_right, and wit_crispr_WT_right. (The full sequence of the corresponding primers can be found in Table S2.) Separate PCR reactions were used to verify each side of the mutation: left arm by wit_crispr_conf_right and wit_outside_1_for and sequenced with wit_outside_1_for, and right arm by wit_crispr_conf2_rev and wit_outside_2_rev and sequenced with wit_outside_2_rev.

Creation of rescue constructs

The entire *wit* locus was amplified using the primers wit_locus_left and wit_locus_right from gDNA and purified by phenyl-chloroform extraction and then cloned into pCR8. An FRT variant of the locus was amplified using the primers wit_locus_L_FRT and wit_locus_R_FRT. These flies were subsequently balanced to a fly that contained a nos:ϕC31 on the X chromosome (Bloomington *Drosophila* Stock Center, 34771). The full sequence of the corresponding primers can be found in Table S3.

Gibson assemblies were conducted using NEB HiFi Assembly Master Mix (2621S) containing 10 fmol of each fragment in a 10 µl reaction. Assemblies created a circular product with the vector backbone pSC. pSC is a linear PCR product of the primers pSC_F and pSC_R, using a pSC cloning kit template (Stratagene, 240205). Assemblies were cloned and screened by restriction fragment mapping in DH10B *Escherichia coli* with *Eco*RI (NEB, R3101S) or *Eco*RV (NEB, R3195S). Assembly of a *D. melanogaster wit* locus with a substituted *D. virilis* SMAD binding site utilized the primers pSC2vir_wit_L_F, vir_wit_L2R_R, vir_wit_R2L_F and vir_wit_R2pSC_R. Assembly of a CFP fusion of WIT utilized the primers wit_locus_left_R, wit_locus_right_F, pSC2vir_wit_L_F, vir_wit_R2pSC_R, wit_CFP_F and wit_CFP_R. The insertion site of CFP followed the signal polypeptide as predicted computationally (Tamura et al., 2011). A deleted SMAD locus was created utilizing the primers pSC2vir_wit_L_F, vir_wit_R2pSC_R, assembly_delSmad_for and assem_dSmad_rev_sho. See Fig. S4 for diagrams of all wit rescue constructs. Primer sequences can be found in Table S3.

The donor vector, pGE-attB-GMR_GW, was created by modifying pGE-attB-GMR (Huang et al., 2009) in order to add a Gateway cloning cassette. This was accomplished by digestion with *Eco*RI (NEB, R3101S) and *Kpn*I (NEB, R3142S), followed by Gibson assembly of a PCR-amplified Gateway cassette with gggcgcgtactccacGTTTATCACCACTTTGTACAAG and catacattatacgaagttatGTTTATCACAAGTTTGTACAAAAAAG. The opposite Gateway cassette was used to make pGE-attB-GRM_GWflip. Mutant loci were subcloned with wit_locus primers including or excluding FRT sites into pCR8 and LR recombined into pGE-attB-GMR. Loci were gateway assembled such that the rescue fragment was in the same orientation as *wit*. Destination vectors were injected into null flies containing nos:ϕC31 and positive flies were selected by expression of red pigmentation in the eye (Bloomington *Drosophila* Stock Center, 34771).

In situ hybridization, immunofluorescence and microscopy

Species-specific cDNA libraries were constructed and *wit* was amplified using the degenerate primers reported previously (Marmion et al., 2013). *In situ* hybridization was performed as reported previously (Niepielko et al., 2014). Dissections and fixation were performed as reported by others (Pacquelet and Rørth, 2005). We reduced the times for dissection and

Development (2018) 145, dev161083. doi:10.1242/dev.161083

permeabilization by half in order to detect proteins with high turnover rate or low abundance at the cell membrane. Specifically, four flies were dissected at a time and moved into a fixation solution. After four cycles, the fixation solution was replaced with a fresh solution, and an additional 10 min of fixation was completed before washes. Primary antibodies were: mouse anti-Wit [23C7; 1:500, Developmental Studies Hybridoma Bank (DSHB)], rabbit anti-phosphorylated-Smad1/5/8 (1:3000, a generous gift from D. Vasiliauskas, S. Morton, T. Jessell and E. Laufer, Columbia University, NY, USA), mouse anti-β-galactosidase (1:1000, Promega, Z3781), rabbit anti-β-galactosidase (1:1000, Invitrogen, A-11132) and sheep anti-GFP (1:2000, Biogenesis, AHP2984). Secondary antibodies were Alexa Fluor 488-, 568- and 647- conjugated (1:1000, Molecular Probes, A-21206, A-21202, A-11015, A10042, A10037 and A-31571). DAPI (1:10,000, Invitrogen, D1306) was used to stain nuclei. Images were captured with a Leica SP8 Confocal microscope. Images were processed with ImageJ (Rasband, 1997–2009) and Gimp (GNU Image Manipulation Program, 1995–2008). The intensity of the vir2 reporter line was measured by a box on the lateral edge of approximately ten cells wide and four cells tall (marked in Fig. 3B,D). A plot profile of intensity was measured from the anterior boundary of the oocyte-associated follicle cells into the main body follicle cells (ImageJ), and expressed in arbitrary units (a.u.). All statistical analysis was conducted with unpaired two-tailed *t*-tests. Sample sizes are indicated in figure panels.

Acknowledgements

We thank V. Veikkolainen and G. Pyrowolakis for continued discussions, and greatly appreciate G. Pyrowolakis for his careful reading of the manuscript. We also thank the members of the Yakoby Lab for insightful discussions. We are grateful to D. Vasiliauskas, S. Morton, T. Jessell and E. Laufer for providing the P-SMAD antibody. We are thankful for the *Drosophila* species fly stock of *D. virilis* and the Developmental Studies Hybridoma Bank for antibodies.

Competing interests

The authors declare no competing or financial interests.

Author contributions

Conceptualization: R.A.M., N.Y.; Methodology: R.A.M.; Formal analysis: R.A.M., N.Y.; Investigation: R.A.M.; Resources: R.A.M.; Writing - original draft: R.A.M., N.Y.; Writing - review & editing: R.A.M., N.Y.; Supervision: N.Y.; Project administration: N.Y.; Funding acquisition: N.Y.

Funding

R.A.M. was partially supported by the Center for Computational and Integrative Biology at Rutgers-Camden (Rutgers, The State University of New Jersey). N.Y. was also supported by a National Science Foundation CAREER Award (IOS-1149144) and by the National Institute of General Medical Sciences (2R15GM101597-02). Deposited in PMC for release after 12 months.

Supplementary information

Supplementary information available online at
http://dev.biologists.org/lookup/doi/10.1242/dev.161083.supplemental

References

Aberle, H., Haghighi, A. P., Fetter, R. D., McCabe, B. D., Magalhães, T. R. and Goodman, C. S. (2002). wishful thinking encodes a BMP type II receptor that regulates synaptic growth in Drosophila. *Neuron* **33**, 545-558.

Ashe, H. L. and Briscoe, J. (2006). The interpretation of morphogen gradients. *Development* **133**, 385-394.

Bastock, R. and St Johnston, D. (2008). Drosophila oogenesis. *Curr. Biol.* **18**, R1082-R1087.

Berg, C. A. (2005). The shell game: patterning genes and morphological change. *Trends Genet.* **21**, 346-355.

Campbell, G. and Tomlinson, A. (1999). Transducing the Dpp morphogen gradient in the wing of Drosophila: regulation of Dpp targets by brinker. *Cell* **96**, 553-562.

Chen, Y. and Schüpbach, T. (2006). The role of brinker in eggshell patterning. *Mech. Dev.* **123**, 395-406.

Crickmore, M. A. and Mann, R. S. (2006). Hox control of organ size by regulation of morphogen production and mobility. *Science* **313**, 63-68.

Dahmann, C., Oates, A. C. and Brand, M. (2011). Boundary formation and maintenance in tissue development. *Nat. Rev. Genet.* **12**, 43-55.

Deng, W. M. and Bownes, M. (1997). Two signalling pathways specify localised expression of the Broad-Complex in Drosophila eggshell patterning and morphogenesis. *Development* **124**, 4639-4647.

Fuchs, A., Cheung, L. S., Charbonnier, E., Shvartsman, S. Y. and Pyrowolakis, G. (2012). Transcriptional interpretation of the EGF receptor signaling gradient. *Proc. Natl. Acad. Sci. USA* **109**, 1572-1577.

Gratz, S. J., Ukken, F. P., Rubinstein, C. D., Thiede, G., Donohue, L. K., Cummings, A. M. and O'Connor-Giles, K. M. (2014). Highly specific and efficient CRISPR/Cas9-catalyzed homology-directed repair in Drosophila. *Genetics* **196**, 961-971.

Hamaratoglu, F., Affolter, M. and Pyrowolakis, G. (2014). Dpp/BMP signaling in flies: from molecules to biology. *Semin. Cell Dev. Biol.* **32**, 128-136.

Hinton, H. E. (1981). *Biology of Insect Eggs*. Oxford: Pergamon Press.

Horne-Badovinac, S. and Bilder, D. (2005). Mass transit: epithelial morphogenesis in the Drosophila egg chamber. *Dev. Dyn.* **232**, 559-574.

Housden, B. E., Valvezan, A. J., Kelley, C., Sopko, R., Hu, Y., Roesel, C., Lin, S., Buckner, M., Tao, R., Yilmazel, B. et al. (2015). Identification of potential drug targets for tuberous sclerosis complex by synthetic screens combining CRISPR-based knockouts with RNAi. *Sci. Signal.* **8**, rs9.

Huang, J., Zhou, W., Dong, W., Watson, A. M. and Hong, Y. (2009). Directed, efficient, and versatile modifications of the Drosophila genome by genomic engineering. *Proc. Natl. Acad. Sci. USA* **106**, 8284-8289.

Jia, D., Tamori, Y., Pyrowolakis, G. and Deng, W.-M. (2014). Regulation of broad by the Notch pathway affects timing of follicle cell development. *Dev. Biol.* **392**, 52-61.

Jordan, K. C., Hatfield, S. D., Tworoger, M., Ward, E. J., Fischer, K. A., Bowers, S. and Ruohola-Baker, H. (2005). Genome wide analysis of transcript levels after perturbation of the EGFR pathway in the Drosophila ovary. *Dev. Dyn.* **232**, 709-724.

Kirkpatrick, H., Johnson, K. and Laughon, A. (2001). Repression of dpp targets by binding of brinker to mad sites. *J. Biol. Chem.* **276**, 18216-18222.

Konikoff, C. E., Karr, T. L., McCutchan, M., Newfeld, S. J. and Kumar, S. (2012). Comparison of embryonic expression within multigene families using the FlyExpress discovery platform reveals more spatial than temporal divergence. *Dev. Dyn.* **241**, 150-160.

Kumar, S., Konikoff, C., Sanderford, M., Liu, L., Newfeld, S., Ye, J. and Kulathinal, R. J. (2017). FlyExpress 7: an integrated discovery platform to study coexpressed genes using in situ hybridization images in Drosophila. *G3 (Bethesda)* **7**, 2791-2797.

Mantrova, E. Y., Schulz, R. A. and Hsu, T. (1999). Oogenic function of the myogenic factor D-MEF2: negative regulation of the decapentaplegic receptor gene thick veins. *Proc. Natl. Acad. Sci. USA* **96**, 11889-11894.

Marmion, R. A., Jevtic, M., Springhorn, A., Pyrowolakis, G. and Yakoby, N. (2013). The Drosophila BMPRII, wishful thinking, is required for eggshell patterning. *Dev. Biol.* **375**, 45-53.

Marqués, G., Bao, H., Haerry, T. E., Shimell, M. J., Duchek, P., Zhang, B. and O'Connor, M. B. (2002). The Drosophila BMP type II receptor Wishful Thinking regulates neuromuscular synapse morphology and function. *Neuron* **33**, 529-543.

Moussian, B. and Roth, S. (2005). Dorsoventral axis formation in the Drosophila embryo–shaping and transducing a morphogen gradient. *Curr. Biol.* **15**, R887-R899.

Müller, B., Hartmann, B., Pyrowolakis, G., Affolter, M. and Basler, K. (2003). Conversion of an extracellular Dpp/BMP morphogen gradient into an inverse transcriptional gradient. *Cell* **113**, 221-233.

Neuman-Silberberg, F. S. and Schupbach, T. (1994). Dorsoventral axis formation in Drosophila depends on the correct dosage of the gene gurken. *Development* **120**, 2457-2463.

Niepielko, M. G., Hernáiz-Hernández, Y. and Yakoby, N. (2011). BMP signaling dynamics in the follicle cells of multiple Drosophila species. *Dev. Biol.* **354**, 151-159.

Niepielko, M. G., Ip, K., Kanodia, J. S., Lun, D. S. and Yakoby, N. (2012). Evolution of BMP signaling in Drosophila oogenesis: a receptor-based mechanism. *Biophys. J.* **102**, 1722-1730.

Niepielko, M. G., Marmion, R. A., Kim, K., Luor, D., Ray, C. and Yakoby, N. (2014). Chorion patterning: a window into gene regulation and Drosophila species' relatedness. *Mol. Biol. Evol.* **31**, 154-164.

Pacquelet, A. and Rørth, P. (2005). Regulatory mechanisms required for DE-cadherin function in cell migration and other types of adhesion. *J. Cell Biol.* **170**, 803-812.

Parker, L., Stathakis, D. G. and Arora, K. (2004). Regulation of BMP and activin signaling in Drosophila. *Prog. Mol. Subcell. Biol.* **34**, 73-101.

Peri, F. and Roth, S. (2000). Combined activities of Gurken and decapentaplegic specify dorsal chorion structures of the Drosophila egg. *Development* **127**, 841-850.

Pyrowolakis, G., Hartmann, B., Müller, B., Basler, K. and Affolter, M. (2004). A simple molecular complex mediates widespread BMP-induced repression during Drosophila development. *Dev. Cell* **7**, 229-240.

Raftery, L. A. and Sutherland, D. J. (1999). TGF-beta family signal transduction in Drosophila development: from Mad to Smads. *Dev. Biol.* **210**, 251-268.

Ren, X., Sun, J., Housden, B. E., Hu, Y., Roesel, C., Lin, S., Liu, L.-P., Yang, Z., Mao, D., Sun, L. et al. (2013). Optimized gene editing technology for Drosophila melanogaster using germ line-specific Cas9. *Proc. Natl. Acad. Sci. USA* **110**, 19012-19017.

Development (2018) 145, dev161083. doi:10.1242/dev.161083

Revaitis, N. T., Marmion, R. A., Farhat, M., Ekiz, V., Wang, W. and Yakoby, N. (2017). Simple expression domains are regulated by discrete CRMs during Drosophila oogenesis. *G3 (Bethesda)* **7**, 2705-2718.

Spradling, A. C. (1993). *Developmental genetics of oogenesis*. In *The Development of Drosophila melanogaster* (ed. M. Bate and A. Martinez-Arias), pp. 1-70. Plainview, NY: Cold Spring Harbor Laboratory Press.

Tamura, K., Peterson, D., Peterson, N., Stecher, G., Nei, M. and Kumar, S. (2011). MEGA5: molecular evolutionary genetics analysis using maximum likelihood, evolutionary distance, and maximum parsimony methods. *Mol. Biol. Evol.* **28**, 2731-2739.

Theodosiou, N. A. and Xu, T. (1998). Use of FLP/FRT system to study Drosophila development. *Methods* **14**, 355-365.

Twombly, V., Blackman, R. K., Jin, H., Graff, J. M., Padgett, R. W. and Gelbart, W. M. (1996). The TGF-beta signaling pathway is essential for Drosophila oogenesis. *Development* **122**, 1555-1565.

Weiss, A., Charbonnier, E., Ellertsdóttir, E., Tsirigos, A., Wolf, C., Schuh, R., Pyrowolakis, G. and Affolter, M. (2010). A conserved activation element in BMP signaling during Drosophila development. *Nat. Struct. Mol. Biol.* **17**, 69-76.

Wolpert, L. (1989). Positional information revisited. *Development* **107**, 3-12.

Wu, M. Y. and Hill, C. S. (2009). Tgf-beta superfamily signaling in embryonic development and homeostasis. *Dev. Cell* **16**, 329-343.

Xi, R., McGregor, J. R. and Harrison, D. A. (2003). A gradient of JAK pathway activity patterns the anterior-posterior axis of the follicular epithelium. *Dev. Cell* **4**, 167-177.

Yakoby, N., Bristow, C. A., Gong, D., Schafer, X., Lembong, J., Zartman, J. J., Halfon, M. S., Schüpbach, T. and Shvartsman, S. Y. (2008a). A combinatorial code for pattern formation in Drosophila oogenesis. *Dev. Cell* **15**, 725-737.

Yakoby, N., Lembong, J., Schupbach, T. and Shvartsman, S. Y. (2008b). Drosophila eggshell is patterned by sequential action of feedforward and feedback loops. *Development* **135**, 343-351.

Zhang, H., Levine, M. and Ashe, H. L. (2001). Brinker is a sequence-specific transcriptional repressor in the Drosophila embryo. *Genes Dev.* **15**, 261-266.